

Strain induced edge magnetism at the zigzag edge of a graphene quantum dot

Shuai Cheng,¹ Jinming Yu,¹ Tianxing Ma,^{1,2,*} and N. M. R. Peres³

¹*Department of Physics, Beijing Normal University, Beijing 100875, China*

²*Beijing Computational Science Research Center, Beijing 100084, China*

³*Centro de Física and Departamento de Física, Universidade do Minho, Campus de Gualtar, Braga 4710-057, Portugal*

We study the temperature dependent magnetic susceptibility of a strained graphene quantum dot using the determinant quantum Monte Carlo method. Within the Hubbard model on a honeycomb lattice, our unbiased numerical results show that a relative small interaction U may lead to a edge ferromagnetic-like behavior in the strained graphene quantum dot. Around half filling, the ferromagnetic fluctuations at the zigzag edge are strengthened both by the on-site Coulomb interaction and the strain, especially in low temperature region.

I. INTRODUCTION

Graphene-based systems have been the subject of a considerable body of research^{1–5} due to their potential application in nano-electronic devices^{6–17}. A perfect graphene sheet consists of a single layer of carbon atoms arranged in a honeycomb crystal lattice as depicted in Fig. 1. Since its discovery, graphene research expanded quickly, and graphene-based systems with different edge topology have been synthesised. It has been suggested that the electronic properties of graphene quantum dots with different edges may find interesting applications in nano-electronic devices, where their edge structure – zigzag, armchair, or something in between – will provide different routes to specific applications. The graphene-based quantum dot depicted in Fig. 1 shows two different types of edges – zig-zag and armchair. For a graphene nanoribbon one can assume it to be infinite in one direction but finite in the perpendicular one. In this way one can produce graphene nanoribbons with either zigzag or armchair terminations³. For a quantum dot, and excluding very specific cases, one always have, at least, the two types of terminations present. That is the case we consider in this paper.

The possibility magnetism in graphene-based materials is an important problem and may open new avenues toward the development of spintronics^{9–13,15–18}. In general, spintronics¹⁹ requires a semiconductor material with some type of magnetic property at (or above) room temperature²⁰. In perfect graphene, it was suggested that antiferromagnetic correlations dominate around half filling, and ferromagnetic fluctuations may dominate in a rather high filling (doped) region around the Van Hove singularity in the density of state²¹. Unfortunately this level of doping is still far from the current experimental ability to dope the material^{22,23}. The possible ferromagnetic order that was proposed to exist in graphene-based materials with defects, such as vacancies, topological defects, and hydrogen chemisorption, are all waiting for experimental confirmation^{24–26}.

Graphene nanoribbons' magnetism has also attracted considerable attention, since it holds promises of many applications in the design of nanoscale magnetic and spintronics devices. It has been shown that the zigzag

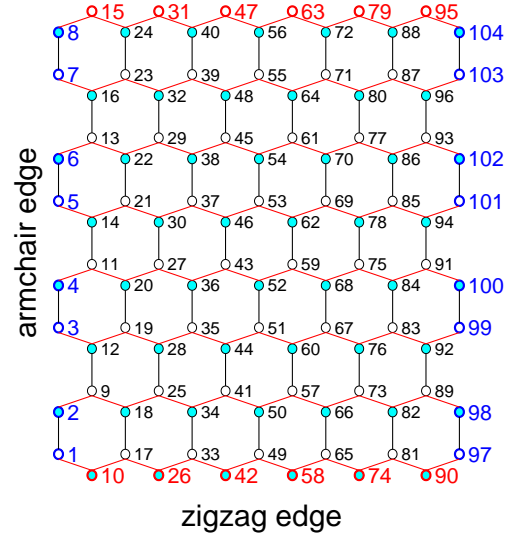


FIG. 1. (Color online) A sketch for a graphene quantum dot with 104 sites where white and cyan circles indicates A and B sublattice respectively. The sites at zigzag edge are marked by red color numbers and the sites at armchair edge are marked by blue color numbers. We consider the strain along the zigzag-direction. The dark line indicates $t_1 = t$, red lines indicates $t_2 = t_3 = t - \Delta t$. Here t represents the nearest hopping term and Δt represents the effect of strain.

graphene nanoribbons exhibit ferromagnetic correlations along the edge at half filling²⁷, and that armchair graphene nanoribbons have ferromagnetic fluctuations in the doped region around the nearly flat band²⁸.

The shape and symmetry of the dots play an important role in the energy level statistics and in the spatial charge density^{30,31}. These properties, spur the interest in magnetism in graphene quantum dots. The tight-binding description of graphene quantum dots reveals that the structure of the edge-state spectrum and the magnetic response of the dots is strongly dependent on the geometric shape of the cluster. Indeed, it exists the possibility of crossover between paramagnetic and diamagnetic responses of the system as a function of its shape, size, and temperature³². The possibility of ground state magnetization in strained graphene quantum dots was suggested

by mean-field calculations²⁹, which revealed that magnetism can be enhanced by as much as 100% for strain values on the order of 20%.

The mean field results show that the critical Hubbard interaction U_c for bulk graphene (unstrained) is about $2.23t$, where t is the nearest hopping term of the honeycomb lattice. This value of U_c put the system into a moderate correlated regime, as U_c is near to the half bandwidth w , where w is about $6t$ ²¹. For such a U_c value, the mean field method may lead to spurious results because the system is very sensitive to the approximation used. The temperature dependent magnetic susceptibility plays a key role in understanding the behavior of magnetism and is used in this paper as a probe to magnetic correlations in graphene quantum dots.

In this paper, using an unbiased numerical method, we study the temperature dependent magnetic susceptibility in a strained graphene quantum dot.

II. MODEL AND METHODS

Strain is an active topic of experimental research both in semiconductors in general and in graphene-based materials. Some degree of strain can be induced either by deposition of oxide capping layers or by mechanical methods²⁹. In the present work, we concentrate on the half-filled and low doping regimes of a graphene quantum dot, a doping level that can be easily realized in experiments²³. Our numerical results reveal a high-temperature ferromagnetic-like behavior at the edges of a strained graphene quantum dot, for reasonable interaction electron-electron interaction values. Such ferromagnetic correlations are enhanced by increasing both the strain and the interaction strength.

Fig. 1 depicts the system under study, which is an honeycomb lattice with 8×13 sites. We can change the size of lattice by changing the length along each edge. The sites at armchair edges have been marked with blue numbers and the sites at the zig-zag ones have been marked with red numbers.

The Hamiltonian for a strained graphene quantum dot can be expressed as

$$H = \sum_{i\eta\sigma} t_{\eta} a_{i\sigma}^{\dagger} b_{i+\eta\sigma} + h.c. + U \sum_i (n_{ai\uparrow} n_{ai\downarrow} + n_{bi\uparrow} n_{bi\downarrow}) + \mu \sum_{i\sigma} (n_{ai\sigma} + n_{bi\sigma}) \quad (1)$$

Here, $a_{i\sigma}$ ($a_{i\sigma}^{\dagger}$) annihilates (creates) electrons at site \mathbf{R}_i with spin σ ($\sigma = \uparrow, \downarrow$) on sublattice A, as well as $b_{i\sigma}$ ($b_{i\sigma}^{\dagger}$) acting on electrons of sublattice B, $n_{ai\sigma} = a_{i\sigma}^{\dagger} a_{i\sigma}$ and $n_{bi\sigma} = b_{i\sigma}^{\dagger} b_{i\sigma}$. U is the on-site Hubbard interaction and μ is the chemical potential. On such honeycomb lattice, t_{η} denotes the nearest neighbor hopping integral. We consider that stress is applied along the zigzag direction. The applied stress modifies the interatomic distances, which

in turn implies a change in the electronic-hopping parameters t_{η} . As a consequence of these changes the band structure of the material is modified. The quantitative change in the hoppings upon stress was studied using ab initio methods, and we illustrate that in Fig. 1. The lines in dark indicating hopping terms with $t_1 = t$ along the direction of stress, which do not change in value. The lines in red change their values as $t_{2,3} = t - \Delta t$, according to the strength of stress parametrized by Δt .

The nearest-neighbor hopping energy t reported in the literature³ ranges from 2.5 to 2.8 eV, and the value of the on-site repulsion U can be taken from its estimation in polyacetylene^{3,33,34} $-U \cong 6.0-17$ eV, which clearly spans a large range of values.

In principle it is questionable to apply for correlated electrons in graphene the simplest version of the Hubbard model with values of U valid for polyacetylene. However, the Peierls-Feynman-Bogoliubov variational principle shows that a generalized Hubbard model with non-local Coulomb interactions is mapped onto an effective Hubbard model with on-site effective interaction U only, which is about $1.6|t|$ ³⁵. Following the latter reference we study the the model Hamiltonian in the range of $U/|t| = 1 - 3$. Although the value of $U/|t| = 3$ is larger than $1.6|t|$, our aim is to explore the importance of interactions on the magnetism of quantum dot under study.

For such ranges of U and t , the the determinant quantum Monte Carlo (DQMC) simulation is a reliable tool for investigating the nature of magnetic correlations in the presence of moderate Coulomb interactions. This is specially true in what concerns changes of the band structure with respect to modifications of transverse width and to the edge topology.

In DQMC, the basic strategy is to express the partition function as a high-dimensional integral over a set of random auxiliary fields. Then the integral is accomplished by Monte Carlo techniques. In present simulations, 8000 sweeps were used to equilibrate the system, and an additional 30000 sweeps were made, each of which generated a measurement. These measurements were split into ten bins which provide the basis of coarse-grain averages, and errors were estimated based on standard deviations from the average. For more technique details, we refer to Refs.^{36,37}.

III. RESULTS

To explore the behavior of magnetism in the graphene quantum dot, we calculate the uniform magnetic susceptibility χ for the bulk, the magnetic susceptibility χ_a at the armchair edge and the magnetic susceptibility χ_z at the zigzag edge. Here

$$\chi = \int_0^{\beta} d\tau \sum_{d,d'=a,b} \sum_{i,j} \langle m_{id}(\tau) \cdot m_{jd'}(0) \rangle \quad (2)$$

where $m_{i_a}(\tau) = e^{H\tau} m_{i_a}(0) e^{-H\tau}$ with $m_{i_a} = a_{i\uparrow}^\dagger a_{i\uparrow} - a_{i\downarrow}^\dagger a_{i\downarrow}$ and $m_{i_b} = b_{i\uparrow}^\dagger b_{i\uparrow} - b_{i\downarrow}^\dagger b_{i\downarrow}$. We measure χ in unit of $|t|^{-1}$. The χ of the bulk is calculated by summing over all the sites. The χ_a at the armchair edge is calculated by summing over the sites marked with red-color numbers in Fig. 1, and the χ_z at the zigzag edge is calculated by summing over the sites marked with blue-color numbers in the same figure. An average for χ , χ_a , and χ_z is made corresponding to the respective total number of sites.

Firstly we present the temperature dependent χ , χ_a , and χ_z for $U = 3.0|t|$, $\langle n \rangle = 1.0$, and $\Delta t = 0.30t$ in Fig. 2. To qualitatively estimate the behavior of the temperature dependence of the magnetic susceptibility, we plot the function $y = 1/x$, since the Curie-Weiss law $-\chi = C/(T - T_c)$ describes the magnetic susceptibility χ for a ferromagnetic material in the temperature region above the Curie temperature T_c .

We note that the χ_z (red circles) increases as the temperature decreases, which shows a ferromagnetic-like behavior. Interesting enough, the χ_a decreases as the temperature decreases. As χ_z is much larger than the χ_a , the bulk uniform magnetic susceptibility χ also increases as the temperature decreases, especially in low temperature region. Within our numerical results, we fit the DQMC data with a formula of

$$\chi_z(T) = a/(T - T_c) + b \quad (3)$$

as that shown (dashed lines) in Fig. 2 which allows to estimate the transition temperature T_c . The fitting agrees with the DQMC data quite well. From this fitting, one may estimate a T_c of about $\sim 0.011t$, which is roughly ~ 320 K. For lower temperatures, one can notice significant error bars on the susceptibility, related to the Monte-Carlo sampling. From Eq. 3, we have

$$T_c = a/[\chi_z(T) - b] + T. \quad (4)$$

To estimate the error bar of the obtained T_c , we use the standard rule for estimating errors of indirect measurement by deriving the partial derivative of the right part of Eq.4, thus obtaining

$$\delta T_c = a \delta \chi_z(T) / \chi_z^2(T). \quad (5)$$

We use the susceptibility at the lowest temperature, T_{lowest} , to estimate the error. We can then estimate $\delta T_c = a \delta \chi_z(T_{lowest}) / \chi_z^2(T_{lowest}) \simeq 0.002|t|$, which indicates that the value of T_c should be statistically distinguishable from zero.

The difference between the temperature dependence of χ_z and χ_a is due to the edge geometry. For an half-filled Hubbard model on a perfect honeycomb lattice, the system shows antiferromagnetic correlations. As the structure of the honeycomb lattice can be described by two inter-penetrating sub-lattices, the spin correlation between the nearest neighbour sites is negative (due to antiferromagnetic correlations), and the spin correlation between the next nearest neighbour sites belonging to the same sub-lattice, has to be positive. In the graphene

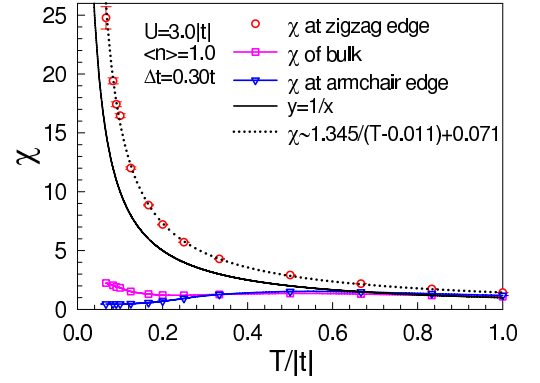


FIG. 2. (Color online) The χ_z (red circles), χ (pink line with square), and χ_a (blue lines with down triangle) as a function of temperature at $U = 3.0|t|$, $\langle n \rangle = 1.0$, and $\Delta t = 0.30t$ of a lattice with 104 sites.

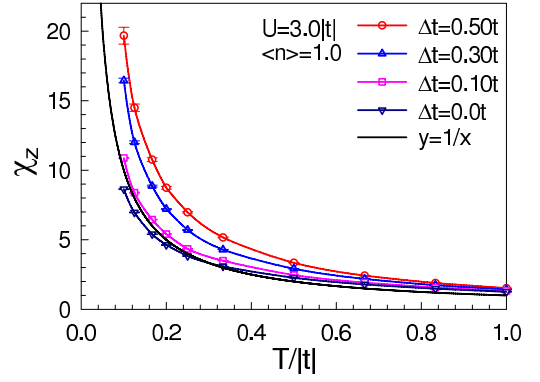


FIG. 3. (Color online) The χ_z at $U = 3.0|t|$ and $\langle n \rangle = 1.0$ with different strain.

dot under study, the sites along the armchair edge belong to different sub-lattices, while the sites along the zig-zag edge belong to the same sublattice. Thus, the magnetic susceptibility at the armchair edge is antiferromagnetic-like while the magnetic susceptibility at the zigzag edge is ferromagnetic-like. As noted already, the susceptibility at the armchair edge is a non-monotonic function of temperature. This may be caused by the competition between the enhanced spin polarization with lowering temperature and unbalanced distribution of electron with different spins at armchair and zigzag edges.

For shedding light on the importance of strain, we present the temperature dependent χ_z at different strain values in Fig. 3. It is clear seen that the χ_z is largely enhanced by strain. The strain decreases the value of t , and thus enhances the effective strength of electron-electron interactions U/t . As a consequence we expect that edge magnetism should be enhanced by strain. This edge-state magnetism has already been detected by scanning tunnelling microscopy²⁷.

In the calculations we have done, the variation of hopping parameters depends on the amount of strain, which is a function of the lattice deformation. The variation of

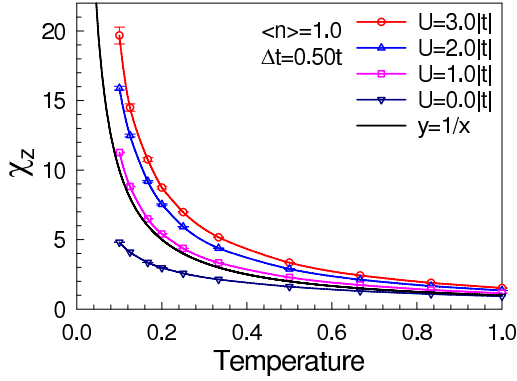


FIG. 4. (Color online) The χ_z at $\Delta t = 0.50t$ and $\langle n \rangle = 1.0$ with different U , which shows that the χ_z is enhanced greatly as the interaction U increases, and as $U \geq 1.0|t|$, a possible ferromagnetic-like behavior is predicted where the χ_z tends to diverge at a relative low temperature.

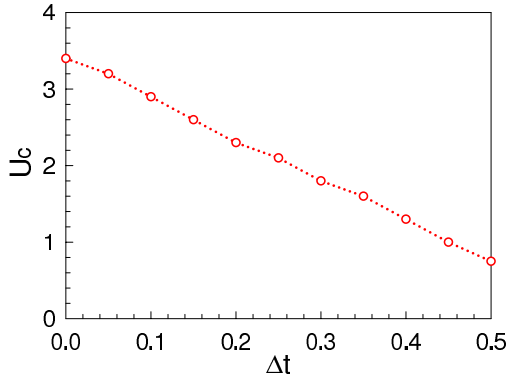


FIG. 5. (Color online) The critical interaction U_c as a function of strain.

the hopping parameters dependence on lattice deformation has been studied using first-principles calculations for a wide range lattice deformations³⁸. From the results published in the literature^{38,39}, one may estimate that $\Delta t = 0.3t$ corresponds to deformation $e = dL/L = 15\%$. Both *ab-initio* calculation⁴⁰ and experiments⁴¹ show that graphene can sustain reversible deformations of the order of 20%, which corresponds to $\Delta t = 0.50t$. For the detail discussions on the relationship between Δt and lattice deformation, we refer the readers to Refs. [29, 38, and 39].

For understanding the physics induced by the Coulomb interaction U , we compute χ_z of the graphene quantum dot with 104 sites for different U values. The results are depicted in Fig. 4. We can see that the χ_z is enhanced by as U increases. At $U = 0$, χ_z behaves like that of a paramagnetic system which does not diverge at a finite low temperature, while as $U > 1.0|t|$, a ferromagnetic like behavior is shown for χ_z as χ_z tends to diverge at a relative low temperature. This indicates that edge magnetism can be realized in a strained graphene quantum dot. The physical mechanism that favors ferro-

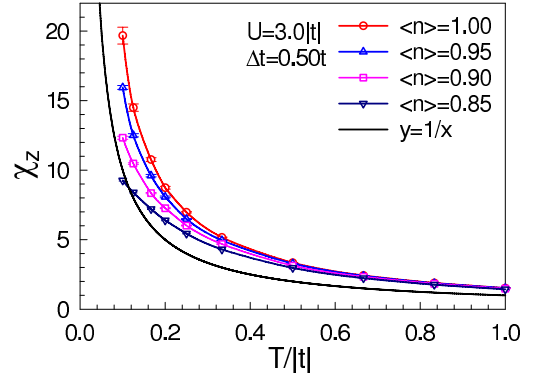


FIG. 6. (Color online) The χ_z at $U = 3.0|t|$ and $\Delta t = 0.50t$ with different $\langle n \rangle$.

magnetic states at zig-zag edges is as follows: the stress along the zig-zag edges tends to produce dimmers weakly coupled between them, which favors a magnetic state at those tightly bound atoms; this contrasts to what happens along the armchair edges. On the temperature dependent magnetic susceptibility at $U = 0$, one can view that the $U = 0$ case as an extension from the small $U > 0$ region.

In Fig. 5, we plot the critical interaction U_c as a function of strain. The U_c decreases as the strain increases, and one may estimate an *optimal* set of parameters as $U = 2.3|t|$ and $\Delta t = 0.20t$, which maybe an ideal value for the experimental realization. Let us now discuss the definition of U_c . For a very large dot, which is almost equivalent to the bulk system, the full symmetry of the honeycomb lattice is restored. In this case a second-order phase transition, at a mean field critical Hubbard interaction, can be defined and used to describe the magnetic transition²⁹. Here, for a finite system, we use the U_c to define the the crossover where the edge magnetic susceptibility may diverge at some value of U and strain. For a fixed strain Δt , we calculate the temperature dependent magnetic susceptibility at different U values and extract the temperature T_c where the magnetic susceptibility may diverge. If the extracted temperature T_c is positive, we define the corresponding lowest U as U_c for a fixed strain Δt .

In Fig. 6, we present χ_z of a graphene quantum dot with 104 sites versus temperature at different electronic fillings $\langle n \rangle$. When the electron filling decreases away from the half filling, χ_z decreases slightly at low temperatures, and the ferromagnetic-like behavior is suppressed when the doping is larger than 10%.

IV. SUMMARY OF RESULTS

In summary, we have studied the edge state magnetism of a strained graphene quantum dot by using the determinant quantum Monte Carlo method. It has been found that the magnetic susceptibility χ_z at the

zigzag edge increases as the temperature decreases. This is specially true in low temperature region. The susceptibility χ_z is markedly strengthened by the on-site Coulomb interaction and is enhanced by strain, which shows a ferromagnetic-like behavior for a relative small Hubbard interaction U with judicious choice of strain. The resultant strongly-enhanced ferromagnetic fluctuations in graphene quantum dots may facilitate the development of many spintronics applications.

ACKNOWLEDGMENTS

T. Ma thanks CAEP for partial financial support. This work is supported by NSFCs (Grant. Nos. 11374034 and 11334012), the Fundamental Research Funds for the Central Universities, and is partially supported by the FEDER COMPETE Program and by the Portuguese Foundation for Science and Technology (FCT) through grant PEST-C/FIS/UI0607/2013. We acknowledge support from the EC under Graphene Flagship (contract no. CNECT-ICT-604391).

-
- * txma@bnu.edu.cn
- ¹ K. S. Novoselov, A. K. Geim, S. V. Morozov, D. Jiang, Y. Zhang, S. V. Dubonos, I. V. Grigorieva, and A. A. Firsov, *Science* **306**, 666 (2004).
 - ² K. S. Novoselov, A. K. Geim, S. V. Morozov, D. Jiang, M. I. Katsnelson, I. V. Grigorieva, S. V. Dubonos, and A. A. Firsov, *Nature (London)* **438**, 197 (2005).
 - ³ A. H. C. Neto, F. Guinea, N. M. R. Peres, K. S. Novoselov, and A. K. Geim, *Rev. Mod. Phys.* **81**, 109 (2009).
 - ⁴ T. Wassmann, A. P. Seitsonen, A. M. Saitta, M. Lazzeri, and F. Mauri, *Phys. Rev. Lett.* **101**, 096402 (2008).
 - ⁵ L. Yang, M. L. Cohen, and S. G. Louie, *Phys. Rev. Lett.* **101**, 186401 (2008).
 - ⁶ X. Yan, X. Cui, B. Li, and Liang-Shi Li, *Nano Lett.* **10**, 1869 (2010).
 - ⁷ O. V. Yazyev and M. I. Katsnelson, *Phys. Rev. Lett.* **100**, 047209 (2008).
 - ⁸ T. Ma, C. Liang, L.-G. Wang, and H.-Q. Lin, *Appl. Phys. Lett.* **100**, 252402 (2012); C. Li, H. Cheng, R. Chen, T. Ma, L.-G. Wang, Y. Song, H.-Q. Lin, *Appl. Phys. Lett.* **103**, 172106 (2013); H. Cheng, C. Li, T. Ma, L.-G. Wang, Y. Song, H.-Q. Lin, *Appl. Phys. Lett.* **105**, 072103 (2014).
 - ⁹ J. Fernandez-Rossier and J. J. Palacios, *Phys. Rev. Lett.* **99**, 177204 (2007).
 - ¹⁰ S. Bhowmick and V. B. Shenoy, *J. Chem. Phys.* **128**, 244717 (2008).
 - ¹¹ J. Jiang, W. Lu, and J. Bernholc, *Phys. Rev. Lett.* **101**, 246803 (2008).
 - ¹² O. V. Yazyev, *Rep. Prog. Phys.* **73**, 056501 (2010).
 - ¹³ N. M. R. Peres, F. Guinea, and A. H. Castro Neto, *Phys. Rev. B* **72**, 174406 (2005).
 - ¹⁴ N. M. R. Peres, *Rev. Mod. Phys.* **82**, 2673 (2010).
 - ¹⁵ M. Sepioni, R. R. Nair, S. Rablen, J. Narayanan, F. Tuna, R. Winpenny, A. K. Geim, and I. V. Grigorieva, *Phys. Rev. Lett.* **105**, 207205 (2010); R. R. Nair, M. Sepioni, I.-L. Tsai, O. Lehtinen, J. Keinonen, A. V. Krashenninnikov, T. Thomson, A. K. Geim, and I. V. Grigorieva, *Nat. Phys.* **8**, 199 (2012).
 - ¹⁶ A. Sharma, V. N. Kotov, and A. H. Castro Neto, *Phys. Rev. B* **87**, 155431 (2013).
 - ¹⁷ B. Roy, F. F. Assaad, and I. F. Herbut, *Phys. Rev. X* **4**, 021042 (2014).
 - ¹⁸ M. Golor, S. Wessel, and M. J. Schmidt, *Phys. Rev. Lett.* **112**, 046601 (2014); J. L. Lado and J. Fernández-Rossier, *Phys. Rev. Lett.* **113**, 027203 (2014).
 - ¹⁹ I. Žutić, J. Fabian and S. Das Sarma, *Rev. Mod. Phys.* **76**, 323 (2004).
 - ²⁰ S. A. Wolf, D. D. Awschalom, R. A. Buhrman, J. M. Daughton, S. von Molnár, M. L. Roukes, A. Y. Chtchelkanova, and D. M. Treger, *Science* **294**, 1488 (2001); K. Ando, *Science* **312**, 1883 (2006).
 - ²¹ T. Ma, F. M. Hu, Z. B. Huang, and H. Q. Lin, *Appl. Phys. Lett.* **97**, 112504 (2010).
 - ²² F. Schedin, A. K. Geim, S. V. Morozov, E. W. Hill, P. Blake, M. I. Katsnelson and K. S. Novoselov, *Nature Materials* **6**, 652 (2007); Y. Zhang, T.-T. Tang, C. Girit, Z. Hao, M. C. Martin, A. Zettl, M. F. Crommie, Y. Ron Shen and F. Wang, *Nature* **459**, 820 (2009).
 - ²³ G. Li, A. Luican, J. M. B. Lopes dos Santos, A. H. Castro Neto, A. Reina, J. Kong and E. Y. Andrei, *Nat. Phys.* **6**, 109 (2010).
 - ²⁴ O. Yazyev *Phys. Rev. Lett.* **101**, 037203 (2008).
 - ²⁵ M. M. Ugeda, I. Brihuega, F. Guinea, and J. M. Gómez-Rodríguez, *Phys. Rev. Lett.* **104**, 096804 (2010).
 - ²⁶ A. J. M. Giesbers, K. Uhlířová, M. Konečný, E. C. Peters, M. Burghard, J. Aarts, and C. F. J. Flipse, *Phys. Rev. Lett.* **111**, 166101 (2013).
 - ²⁷ C. Tao, L. Jiao, O. V. Yazyev, Y.-C. Chen, J. Feng, X. Zhang, R. B. Capaz, J. M. Tour, A. Zettl, S. G. Louie, H. Dai and M. F. Crommie, *Nat. Phys.* **7**, 616 (2011); H. Feldner, Z. Y. Meng, T. C. Lang, F. F. Assaad, S. Wessel, and A. Honecker, *Phys. Rev. Lett.* **106**, 226401 (2011).
 - ²⁸ T. Ma, S. Liu, P. Gao, Z. B. Huang, and H. Q. Lin, *J. Appl. Phys.* **112**, 073922 (2012).
 - ²⁹ J. Viana-Gomes, Vitor M. Pereira, and N. M. R. Peres, *Phys. Rev. B* **80**, 245436 (2009).
 - ³⁰ J. Wurm, A. Rycerz, I. Adagideli, M. Wimmer, K. Richter, and H. U. Baranger, *Phys. Rev. Lett.* **102**, 056806 (2009).
 - ³¹ J. Akola, H. P. Heiskanen, and M. Manninen, *Phys. Rev. B* **77**, 193410 (2008).
 - ³² T. Espinosa-Ortega I. A. Lukyanchuk, and Y. G. Rubo, *Phys. Rev. B* **87**, 205434 (2013).
 - ³³ T. A. Gloor and F. Mila, *Eur. Phys. J. B* **38**, 9 (2004); I. F. Herbut, *Phys. Rev. Lett.* **97**, 146401 (2006).
 - ³⁴ R. G. Parr, D. P. Craig, and I. G. Ross, *J. Chem. Phys.* **18**, 1561 (1950); D. Baeriswyl, D. K. Campbell, and S. Mazumdar, *Phys. Rev. Lett.* **56**, 1509 (1986).
 - ³⁵ M. Schüler, M. Rösner, T. O. Wehling, A. I. Lichtenstein, and M. I. Katsnelson, *Phys. Rev. Lett.* **111**, 036601 (2013).
 - ³⁶ R. Blankenbecler, D. J. Scalapino, and R. L. Sugar, *Phys. Rev. D* **24**, 2278 (1981).
 - ³⁷ T. Ma, F. M. Hu, Z. B. Huang, and H. Q. Lin, *Horizons in World Physics*. **276**, Chapter 8, Nova Science Publishers, Hauppauge, New York, Inc. (2011).

- ³⁸ R. M. Ribeiro, V. M. Pereira, N. M. R. Peres, P. R. Briddon and A. H. Castro Neto, New J. Phys. **11**, 115002(2009).
- ³⁹ V. M. Pereira and A. H. Castro Neto, and N. M. R. Peres, Phys. Rev. B **80**, 045401 (2009).
- ⁴⁰ F. Liu, P. Ming and J. Li, Phys. Rev. B **76** 064120 (2007).
- ⁴¹ Y. Zhao, H. Jang, S. Y. Lee, J. M. Kim, K. S. Kim, J.-H. Ahn, P. Kim, J.-Y. Choi and B. H. Hong, Nature **457**, 706 (2009).